Model Predictive Control for Power System Frequency Control Taking into Account Imbalance Uncertainty [*]

Anne Mai Ersdal [*] **Davide Fabozzi** [**] **Lars Imsland** [*] **Nina F. Thornhill** [**]

[*] *Department of Engineering Cybernetics*
Norwegian University of Science and Technology, Trondheim, Norway
(e-mail: {anne.mai.ersdal,lars.imsland}@itk.ntnu.no).
[**] *Department of Chemical Engineering*
Imperial College London, London, United Kingdom
(e-mail: davide.fabozzi@gmail.com, n.thornhill@imperial.ac.uk).

Abstract: Model predictive control (MPC) is investigated as a control method for frequency control of power systems which are exposed to increasing wind power penetration. For such power systems, the unpredicted power imbalance can be assumed to be dominated by the fluctuations in produced wind power. An MPC is designed for controlling the frequency of wind-penetrated power systems, which uses the knowledge of the estimated worst-case power imbalance to make the MPC more robust. This is done by considering three different disturbances in the MPC: one towards the positive worst-case, one towards the negative worst-case, and one neutral in the middle. The robustified MPC is designed so that it finds an input which makes sure that the constraints of the system are fulfilled in case of all three disturbances. Through simulations on a network with concentrated wind power, it is shown that in certain cases where the state-of-the-art frequency control (PI control) and nominal MPC violate the system constraints, the robustified MPC fulfills them due to the inclusion of the worst-case estimates of the power imbalance.

1. INTRODUCTION

To ensure a stable and secure deliverance of power, it is of vital importance to balance the power demand and supply in a power system. Whenever the demand and supply is out of balance, the frequency of the power system will change, and maintaining this balance is often referred to as *frequency control* (FC). Today, a three-level hierarchical control structure for FC of interconnected power systems is common. These three levels, in increasing hierarchical order, are often referred to as primary, secondary and tertiary control (Machowski et al., 2008). Equivalent, less ambiguous terms have recently been proposed: *frequency containment reserve* (FCR), *frequency restoration reserve* (FRR) and *replacement reserve* (RR) (ENTSO-E, 2012).

Fig. 1 shows the nature of how FCR, FRR and RR cooperate to compensate for a power imbalance. It also shows the timescales of when they are required to activate in the Nordic network. FCR controllers are local, automatic controllers situated at the generating units, and they are required to act instantaneous. The FRR controller is a somewhat slower and centralized, often automated controller that replaces the FCR. Then there is the even slower RR controller, which again replaces the FRR. This is mainly executed manually by the transmission system operators (TSOs).

In the Nordic network, the hydro power generators have historically been the main provider of FCR, while other generating units such as thermal and nuclear power generators as well as
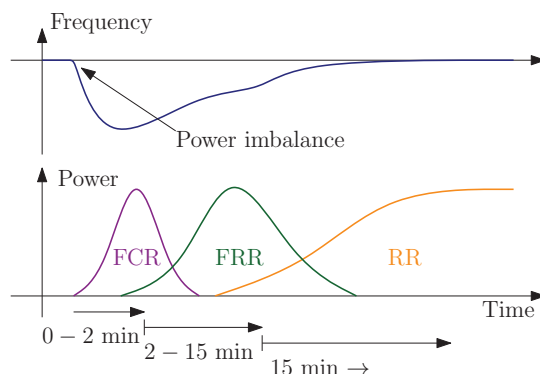
Fig. 1. Activation of FCR, FRR and RR after power imbalance.

some controllable loads participate in RR (Statnett, 2012). In December 2012, the Norwegian operator Statnett became the first of the Nordic TSOs to adopt FRR (Statnett, 2012): the other Nordic operators have introduced similar services in early 2013, and it is likely that both hydro and thermal power generators will provide FRR. Recently, there have also been suggestions on how to include industrial loads in FRR schemes (Fabozzi et al., 2013).

Today, it is mainly proportional-integral (PI) controllers which are applied to FC, and these are tuned based on operator practice (Bevrani, 2009). Fig. 2 shows how the number of *frequency incidents*, i.e. minutes spent outside $49.9 - 50.1$ Hz, has developed concurrently with the wind power penetration in the Nordic network during the last decade. It is clearly increasing, and it can be assumed that today's FC methods are losing their suitability for future power systems. There are several reasons for this development, but two important
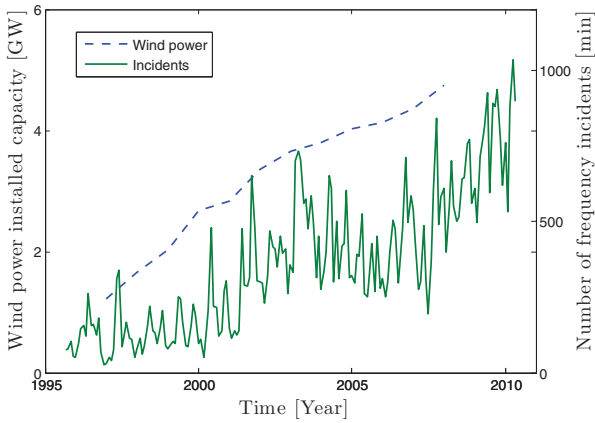
Fig. 2. Installed wind power capacity (Nordel, 2008) and number of frequency incidents per month in the Nordic system (Whitley and Gjerde, 2011).

ones are the network's ability to deal with the intermittency associated with renewable energy resources, especially wind power, and also a heavier loaded network with an increasing amount of bottlenecks (Statnett, 2012). The latter often results in control resources being excluded from participating in FC. It is therefore important to find a control method that in a better way than today plans and executes FC, making the network more robust against intermittent energy resources and also avoiding bottleneck congestions.

Based on these challenges, there has been an increasing interest in applying model predictive control (MPC) to FC during the last decade, some examples being Venkat et al. (2008); Shiroei et al. (2013); Mohamed et al. (2012). Some also consider robust MPC (Shiroei et al., 2013), but this is mainly against system parameters uncertainties, and the fulfillment of system constraints under disturbances is not considered. Other control methods that have been applied for robust FC are H_∞ control (Singh et al., 2013; Bevrani et al., 2011), fuzzy logic (Cam and Kocaarslan, 2013), and also robust PID tuning methods (Khodabakhshian and Edrisi, 2008).

The majority of work that has been published with MPC for FC are based on linear models. In this work, however, the MPC setup allow non-linear models. In addition, the three levels of FC is viewed separately, with distinct governor and turbine models for the FCR, FRR and RR. The MPC implements control of both the FRR and the RR while FCR control is implemented decentralized using local P-controllers. The MPC is robustified against uncertainties in the power imbalance so that the system constraints are fulfilled at all times.

2. SYSTEM MODEL

2.1 System Equations

The model used in this paper is inspired by Bevrani (2009). It is similar to the one used in Ersdal et al. (2013), but here the model is extended to a multiple-area system with n areas connected by tie lines. Fig. 3 shows an example of such a system where $n = 3$. This is a simplified model, where the network and electromechanical dynamics are neglected, which reduce model complexity while retaining the dynamics important for frequency control, as argued in Bevrani (2009). The low complexity model helps to ensure real-time computational properties of the MPC algorithms.
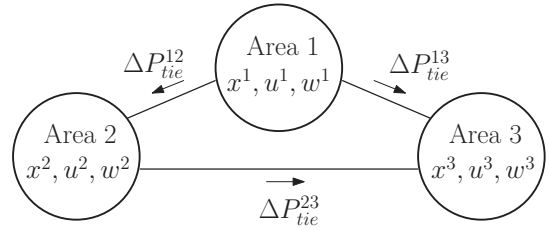

Fig. 3. Multiple-area power system ($n = 3$).

The dynamics of each area i describe the deviation from an initial steady state, and they are represented by the following differential equation (Bevrani, 2009)

$$\frac{d\Delta f^i}{dt} = \frac{1}{2H^i}\left(\Delta P_m^i - \Delta P_L^i - \Delta P_{tie}^i\right) - \frac{D^i}{2H^i}\Delta f^i \quad (1)$$

where Δf^i is the deviation from the nominal frequency f_s, ΔP_m^i the total change in mechanical power from FCR, FRR and RR control combined, ΔP_L^i the electrical power imbalance, ΔP_{tie}^i the change in total power flow from area i on all its tie lines, H^i the inertia of the rotating masses, and D^i the load damping coefficient of the area. The change in total tie-line power flow from area i is given by (Bevrani, 2009)

$$\frac{d\Delta P_{tie}^i}{dt} = 2\pi\left(\Delta f^i \sum_{\substack{j=1\\j\neq i}}^{n} T_{ij} - \sum_{\substack{j=1\\j\neq i}}^{n} T_{ij}\Delta f^j\right) \quad (2)$$

where $\Delta f^{i/j}$ is the local frequency in area i/j, T_{ij} the synchronizing torque coefficient between area i and j, and n the number of areas of the system. If area i and j are not connected by a tie line, then $T_{ij} = 0$. The frequency deviation of the entire system is defined as

$$\Delta f = \frac{\sum_{i=0}^{n} H^i \Delta f^i}{\sum_{i=0}^{n} H^i} \quad (3)$$

The governor/turbines participating at each level of control are gathered into aggregated governor/turbine sets. It is assumed that the FCR, FRR and RR are distributed among the areas, and so there is one aggregated governor/turbine model per control level per area. The FCR-turbines are modeled as simplified hydro turbines (Machowski et al., 2008)

$$\text{Governor: } \Delta P_g(s) = \frac{1+T_{g2}s}{(1+T_{g1}s)(1+T_{g3}s)} \cdot \Delta P_c(s) \quad (4a)$$

$$\text{Turbine: } \Delta P_m(s) = \frac{1-T_t s}{1+0.5T_t s} \cdot \Delta P_g(s) \quad (4b)$$

and the FRR and RR-turbines as thermal units (Bevrani, 2009)

$$\text{Governor: } \Delta P_g(s) = \frac{1}{1+T_g s} \cdot \Delta P_c(s) \quad (5a)$$

$$\text{Turbine: } \Delta P_m(s) = \frac{1}{1+T_t s} \cdot \Delta P_g(s) \quad (5b)$$

where ΔP_c is the control signal to the governor, ΔP_g the valve position from the governor to the turbine, ΔP_m the mechanical power output from the turbine, and T_g and T_t the time constants of the governor and turbine, respectively.

The local FCR controllers are implemented as proportional controllers

$$\Delta P_{c,FCR}^i = -\frac{1}{R}\text{sat}\left(\Delta f^i\right) \quad (6)$$

982

where R is the droop given by the TSO, and sat $\left(\Delta f^i\right)$ is the local frequency saturated at ± 0.1. This is to model full FCR activation at frequency deviations outside ± 0.1 Hz.

The total system can therefore be represented by a nonlinear dynamic equation

$$\dot{\bar{x}} = \bar{f}\left(\bar{x}, \bar{u}, \bar{w}\right). \tag{7}$$

Depending on the number of areas n, the total system consists of $9n$ state variables $\bar{x} = \left[\bar{x}^1 \cdots \bar{x}^n\right]^T$, $2n$ controlled inputs $\bar{u} = \left[\bar{u}^1 \cdots \bar{u}^n\right]^T$, and n disturbances $\bar{w} = \left[\bar{w}^1 \cdots \bar{w}^n\right]^T$, where $\bar{x}^i = \left[\Delta f^i \ \bar{x}_1^i \ \bar{x}_2^i \ \bar{x}_3^i \ \Delta P_{g,FRR}^i \ \Delta P_{m,FRR}^i \ \Delta P_{g,RR}^i \right.$ $\left. \Delta P_{m,RR}^i \ \Delta P_{tie}^i\right]^T$, $\bar{u}^i = \left[\Delta P_{c,FRR}^i \ \Delta P_{c,RR}^i\right]^T$, and $\bar{w}^i = \Delta P_L^i$. The state variables $\bar{x}_1^i$, $\bar{x}_2^i$ and $\bar{x}_3^i$ are the state variables from the hydro turbine and governor transfer functions, from which $\Delta P_{g,FCR}$ and $\Delta P_{m,FCR}$ can be found.

2.2 System disturbance ΔP_L

Most power networks today are market based, and through these markets the predicted power demand and supply are balanced on slots of normally one hour. However, within this hour, there is an unpredicted power imbalance which must be compensated for by the FCR, FRR and RR. In this model the disturbance is this unpredicted power imbalance, and its main component with regards to FC is the difference between power supply and power consumption from intermittent generators and loads, respectively. For each area, this can be summarized into one total load-power imbalance ΔP_L^i.

When dealing with power systems including a certain amount of wind power, such as the Nordic grid, one can for simplicity assume that this unpredicted power imbalance is dominated by the fluctuations in produced wind power. And if in addition it is assumed that the majority of wind power is situated in area m, ΔP_L of all the other areas can be neglected, and the system is affected by one single disturbance $\Delta P_L = \Delta P_L^m$. With the Nordic network in mind, Denmark and South Sweden contribute with about 80% of the total wind power production (Statnett, 2012), and the Nordic network could therefore be a candidate for such a system.

2.3 Delays and Control Signal Dispatching

There are several delays in a power system, and the ones included in this model are presented in the following. There are no delays associated with the FCR, as its control is based on local frequency measurements and it is required to act instantaneously. For the FRR and RR controllers, however, the model implements 40 s delay associated with performing measurements and state estimation, and also delays which represent the time it will take for the FRR and RR turbines to deliver what they are asked. The latter is set to 20 s and 120 s, respectively. All of these delays are known to the MPC.

The FCR control signal is continuous, but the FRR and RR control signals are dispatched at certain intervals and kept constant between the dispatching times. The FRR and RR control signals are dispatched every 10 and 60 s, respectively. MPC provides a flexible framework to implement control with different dispatching frequencies.

3. CONTROLLER

3.1 Control Problem

In order for the system to be operated in a safe and stable manner, the frequency controllers must keep the frequency within a certain bound. As mentioned in Section 1, this includes avoiding bottleneck congestions so that all available reserves are able to participate in stabilizing the frequency.

It is important to distinguish between the need to avoid congestions, and the need to control the power transfer in tie lines. Today it is common to include the deviation in tie-line power transfer from a certain set point in the input to the FRR controller, so that this is restored along with the frequency (Machowski et al., 2008). However, these are cases where it is important that the power exchange between two areas are kept at a given level, for example for economic reasons. In the Nordic network there is a common market, and there are no set points on how much power that should flow from one area to another, as long as bottleneck congestions are avoided. Therefore, setpoints on tie-line power transfer is not implemented here.

There is also the question on the costs connected to FC. In accordance to how fast they are required to activate, the cost of using the reserves are not equal for FCR, FRR and RR: FCR is the most expensive and the RR the least expensive. Another incentive for the controller is therefore to keep the total cost associated with FC at a minimum.

3.2 MPC

MPC is a framework for advanced control, and some of its strengths are that it is optimizing, constraint-handling and exploits disturbance measurements, all of which makes it well suited for FC. MPC uses a model of the system to predict how it will behave in the future, and then optimizes the controlled input with regards to an objective function measuring predicted performance. Mathematically, it can be formulated as a continuous time optimal control problem on the form (8a) subject to (8b) - (8d) (Biegler, 2010)

$$\min_{x(\cdot),u(\cdot)} J\left(x(t), u(t)\right) \tag{8a}$$

$$x(0) - x_0 = 0 \quad \text{Fixed initial state} \tag{8b}$$

$$\dot{x}(t) - f\left(x(t), u(t), \hat{w}(t)\right) = 0 \quad \text{System model} \tag{8c}$$

$$g\left(x(t), u(t)\right) \leq 0 \quad \text{Constraints} \tag{8d}$$

where $x(t)$ are the system states, $u(t)$ the controlled inputs, $\hat{w}(t)$ the predicted disturbances, and $J\left(x(t), u(t)\right)$ the control objective function.

The main idea behind the MPC is to solve an optimization problem at regular time instants to find the optimal system input $u(t)$ over a fixed time horizon with respect to the objective function $J(\cdot)$, and then apply the first part of $u(t)$ as input to the system until next time instant. The control loop is closed by a system measurement $y(t)$. The MPC needs knowledge of the entire initial state vector $x_0 = x(0)$, for which a state estimator may be applied, and also of the predicted system disturbance estimate $\hat{w}(t)$. Here it will be assumed that the entire initial state vector is known. It is also assumed that the current disturbance, $w(0)$, is measured and used as predicted system disturbance.

The system constraints includes limitations on the generation capacity, on the generation rate of change, and also on the power flow in the tie lines connecting the areas of the system. The first two are hard constraints due to physical limitations, and the latter is a softer constraint with a safety margin to the absolute physical transfer limit. However, violating the tie-line constraint may lead to dangerous situations involving overheating etc.
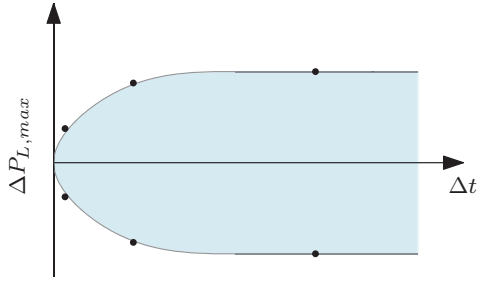
Fig. 4. How a worst-case estimate for ΔP_L could look.

The decision variables, $\Delta P_{c,FRR}^i$ and $\Delta P_{c,RR}^i$, are kept piecewise constant so that they match the control signal dispatching in the system. Matching with Section 2.3, $\Delta P_{c,FRR}^i$ changes every 10 s and $\Delta P_{c,RR}^i$ every 60 s.

The saturation of (6) is nonlinear, implying that we have nonlinear equality constraints (8c), and hence nonlinear MPC (NMPC) must be used. For the same reason, the optimization problem in (8) is non-convex. The continuous time optimization problem (8a) in the NMPC is solved with direct methods, that is, it is discretized and transformed into a nonlinear program (NLP) (Biegler, 2010). In this work collocation has been applied for discretization, and it has been implemented using the CasADi software (Andersson et al., 2012).

Nominal stability of the MPC can be guaranteed through methods described in Grüne and Pannek (2011), that is, either through so-called terminal constraints, or trough finding appropriate stage cost and optimization horizon which under certain assumptions guarantees stability. In this work, we have not considered stability in other ways than choosing a long horizon. While this does not guarantees stability, there are theoretical justifications for doing this (Grüne and Pannek, 2011), and stability is supported by simulations.

3.3 Worst-case estimate of ΔP_L

For different wind farms the worst case variations from the predicted power output can be estimated. For example Holttinen (2004) presents worst-case variations for a specific wind farm within one second, one minute and one hour into the future Δt. Points from several wind farms may be combined and interpolated to create a worst-case estimate for the continuous-time bound of the future power imbalance, see Fig. 4. Given such an estimate, an NMPC which is robustified with regards to such disturbances can be designed.

If the wind farms are distributed more evenly in the system, so that the assumption in Section 2.2 no longer applies, the disturbance would enter at several points and a worst case combination of the disturbances, where system dynamics are considered, has to be calculated.

3.4 Robustified NMPC

Robust NMPC is often approached using the concept of min-max NMPC (Rawlings and Mayne, 2009), which results in large and complex optimization problems. In this work a robustified NMPC (RNMPC) will be applied for FRR and RR control. It is a simplified, nonlinear version of the min-max feedback MPC presented in Scokaert and Mayne (1998), however we do not consider all possible disturbance scenarios, only what we believe to be the worst case, as the one presented in the previous section. There is also resemblance to scenario-based NMPC (Huang et al., 2009; Goodwin and Medioli, 2013).
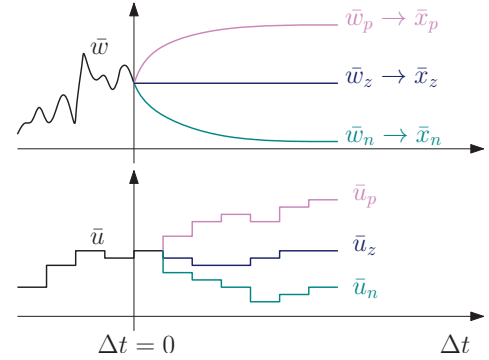

Fig. 5. Sketch of how the robust MPC works. For simplicity, $\bar{u}$ is considered to be scalar.

A new state vector is constructed by combining the original state vector $\bar{x}$ exposed to three different future disturbances: The zero, negative, and positive worst-case estimate for ΔP_L added to the current measured disturbance $\bar{w}_0$, see Fig. 5. Note that neither the robustified nor the nominal NMPC (NNMPC) has any knowledge of the future power imbalance, only a measure of the present one. The system equation for the combined system, which is used in (8c), is then

$$\dot{x} = \begin{bmatrix} \dot{\bar{x}}_z \\ \dot{\bar{x}}_p \\ \dot{\bar{x}}_n \end{bmatrix} = \begin{bmatrix} f\left(\bar{x}_z, \bar{u}_z, \bar{w}_z\right) \\ f\left(\bar{x}_p, \bar{u}_p, \bar{w}_p\right) \\ f\left(\bar{x}_n, \bar{u}_n, \bar{w}_n\right) \end{bmatrix} = f\left(x, u, w\right) \quad (9)$$

where $u = \begin{bmatrix} \bar{u}_z & \bar{u}_p & \bar{u}_n \end{bmatrix}^T$ and $w = \begin{bmatrix} \bar{w}_z & \bar{w}_p & \bar{w}_n \end{bmatrix}^T$. At each optimization it is required that for the first element of $u(t)$, $\bar{u}_z$, $\bar{u}_n$ and $\bar{u}_p$ must be equal. After this, they are free to vary in manners optimal for their designated system states, see Fig. 5. In this way every input guarantees that the optimal input trajectory for all three scenarios, fulfilling all system constraints, are still feasible.

With regards to "nominal" stability of the RNMPC, the fact that "new" disturbance scenarios are considered at each time instant, means that it is not straightforward that the property of recursive feasibility holds, thereby complicating use of standard stability approaches (cf. Section 3.2). However, since the disturbance in step $k+1$ will not be any larger than considered in step k, one would intuitively not expect feasibility problems.

4. SIMULATIONS

4.1 Case Study

A two-area system is considered ($n = 2$), where the majority of wind power production is situated in system 2. As described in Section 2.2, the disturbance in Area 1, ΔP_L^1, is therefore equal to zero, and $\Delta P_L = \Delta P_L^2$. The areas are of equal size with regards to power production, loads, and reserves, and they are connected by a tie line with limited power transfer. This means that the parameters and constraints, which can be seen in Table 1, are equal for the two areas.

The performance of the RNMPC is compared with the NN-MPC, which is based on $\dot{\bar{x}}_z = \bar{f}\left(\bar{x}_z, \bar{u}_z, \bar{w}_z\right)$, and two conventional PI controllers. The controllers are compared against each other by applying a *control performance measure* (CPM). In Gross and Lee (2001) two control performance criteria for FC are presented, which are more general formulations of the performance criteria used by the North American electric reliability corporation (NERC). These are used to ensure a certain quality of the FC by demanding that they stay below a certain

Table 1. System parameters, p.u.-base of 10 GW.

H	0.0835 pu·s	$T_{g,FRR}$	0.08 s
D	0.045 pu/Hz	$T_{t,FRR}$	30 s
T_{12}	0.2 pu/Hz	$T_{g,RR}$	0.08 s
f_s	50 Hz	$T_{t,RR}$	40 s
R	3 Hz/pu	$|\Delta P_{tie}|$	≤ 0.03 pu
$T_{g1,FCR}$	0.5 s	$\left|\Delta P_{c,FRR}\right|$	≤ 0.05 pu
$T_{g2,FCR}$	3 s	$\left|\Delta P_{c,RR}\right|$	≤ 0.25 pu
$T_{g3,FCR}$	50 s	$\left|\Delta \dot{P}_{c,FRR}\right|$	$\leq 2\cdot 10^{-4}$ pu/s
$T_{t,FCR}$	0.5 s	$\left|\Delta \dot{P}_{c,RR}\right|$	$\leq 1\cdot 10^{-4}$ pu/s

value, and they can therefore also be used as a CPM: the lower the CPM, the better. First the average of Δf is calculated over windows of 30 s in order to filter out the fast fluctuations, then the CPM is found by again taking the average of all these windows.

4.2 Tuning the NMPC

The main tuning variables of the NMPC are the prediction horizon for the optimization T and the design of the objective function $J(\cdot)$. The continuous time objective function is

$$J(x,u) = \int_{t=0}^{T} x^T Q x + u^T R u \ dt \qquad (10)$$

where $Q = \text{diag}\left(\bar{Q}_z, \bar{Q}_p, \bar{Q}_n\right)$ and $R = \text{diag}\left(\bar{R}_z, \bar{R}_p, \bar{R}_n\right)$ for RNMPC, and $Q = \bar{Q}$ and $R = \bar{R}$ for NNMPC. Q is real, symmetric and positive semidefinite, while R is real, symmetric and positive definite. Based on the control objectives discussed in Section 3.1, the non-zero elements of the tuning matrices $\bar{Q}$ and $\bar{R}$ were after some trial and error chosen to be $\bar{q}_{11} = \frac{(H^1)^2}{(H^1+H^2)^2}$, $\bar{q}_{99} = \frac{(H^2)^2}{(H^1+H^2)^2}$, $\bar{q}_{19} = q_{91} = \frac{H^1 H^2}{(H^1+H^2)^2}$, $\bar{q}_{ii} = 1$ for $i = \{2\cdots 6, 11\cdots 15\}$, $\bar{r}_{ii} = 1$ for $i = \{1,3\}$, and $\bar{r}_{ii} = 0.01$ for $i = \{2,4\}$. In order to place more emphasis on deviations in $\bar{x}_z$, $\bar{Q}_z$ was set equal to $\bar{Q}$, while $\bar{Q}_p = \bar{Q}_n = 0.1\bar{Q}$. For deviation in inputs, the three systems were all punished equally: $\bar{R}_z = \bar{R}_p = \bar{R}_n = \bar{R}$.

In this way deviation in overall network frequency (3) is punished. Also use of FCR and FRR is punished more than use of RR. The optimization horizon T was chosen to be 3 minutes, a decision based on a compromise between system time constants and complexity.

4.3 Simulations

Case A In Case A, the disturbance (entering in area 2) is at a level such that ΔP_{tie} does not reach its limit, simulation results of Δf can be seen in Fig. 6(a). Fig. 7(a) shows ΔP_{tie}, and it it seen that both the PID and the NNMPC stabilizes ΔP_{tie} at a higher level than the RNMPC, however still with a good clearance to the ΔP_{tie}-limit at 0.03 p.u.

Case B In Case B the initial state of the system has $\Delta P_L \neq 0$ (and thus $\Delta P_{tie} \neq 0$), and after approximately 4 min ΔP_L follows the positive worst-case scenario from Fig. 4. The resulting Δf and tie-line power transfer is displayed in Fig. 6(b) and 7(b), respectively. The latter shows that both the PID and the NNMPC violate the constraint on ΔP_{tie}, while the RNMPC keeps well within. Fig. 8 shows how FRR and RR in the two areas are employed differently with NNMPC and RNMPC.
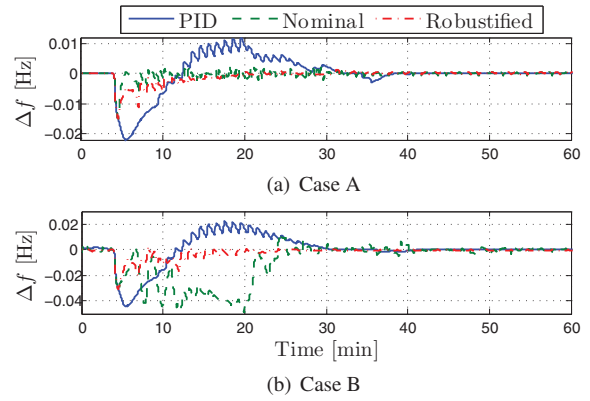

Fig. 6. Δf for all three controllers with disturbance from Case A and B.
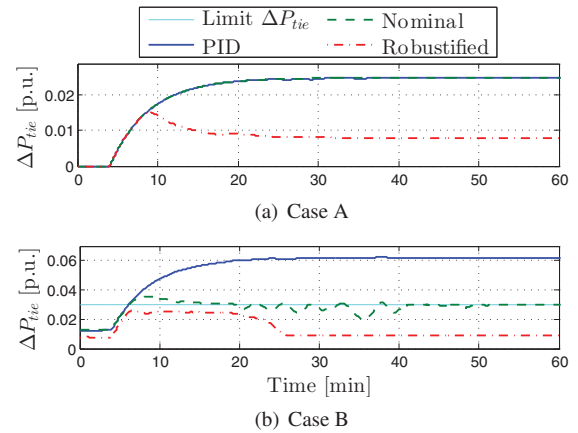

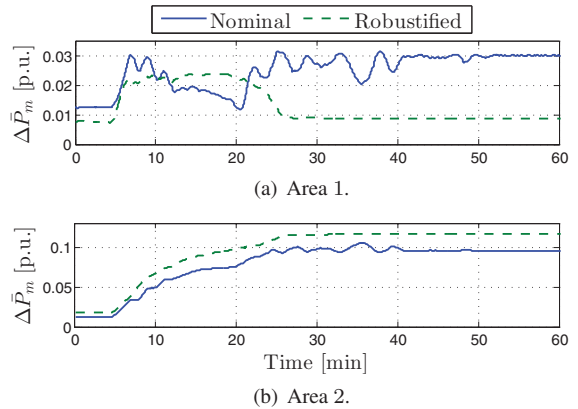Fig. 7. ΔP_{tie} for all three controllers with disturbance from Case A and B.

Fig. 8. Case B: use of $\Delta \bar{P}_m = \Delta P_{m,FRR} + \Delta P_{m,RR}$ in Area 1 and Area 2 with nominal and robustified MPC.

5. DISCUSSION

Ersdal et al. (2013) discussed some of the benefits an NMPC provides with regards to exploiting disturbance measurements, planning ahead, and coordinating system inputs (by automation of FRR and RR control), and in this work the emphasis has been placed on making the NMPC more robust against disturbances dominated by fluctuations in produced wind power. In Ersdal et al. (2013) extensive simulations were carried out that showed an improvement in FC with NMPC, along with lower use of FCR and RR, at the expense of higher use of RR.

Table 2. CPM and reserves usage (given in MWh).

		CPM $(\cdot 10^{-5})$	FCR	FRR	RR
Case A	PI	3.7	22	74	**356**
	Nominal	**0.16**	**2.4**	25	398
	Robustified	0.47	6.8	**23**	397
Case B	PI	14.6	44	146	962
	Nominal	30.9	62	248	**797**
	Robustified	**2.2**	**14.6**	**117**	966

In this work, simulations show that both the PI controller and the NNMPC violate system constraints under severe disturbances, while the RNMPC manages to keep within. From Fig. 7(b), it is seen that with RNMPC less power is transfered between the areas at the initial steady state, i.e. a higher amount of RR is activated in Area 2 than Area 1. This allows for use of the tie-line capacity in times with more urgent transfer needs. Such a situation arises in Case B after approximately 4 minutes, and in Fig. 8 it is seen that compared to the NNMPC the RNMPC is more aggressive in Area 2. This is to compensate for the power imbalance without violating the tie-line power transfer capacity. Since the RNMPC in addition had higher clearance to the transfer limit to begin with, it manages to keep within while the NNMPC does not. Table 2 also shows that in Case B, the RNMPC performs best according to the CPM. It also uses less of the more expensive FCR and RR, but more of the cheaper RR. The NNMPC actually performs worse than the PI, but the constraint violation is much more severe for the PI controller.

When the disturbance is so that the tie-line power transfer constraints are not violated by the NNMPC, as in Case A, the NNMPC performs best. As seen in Table 2, it has the lowest CPM and also the lowest use of FCR. This is not surprising as the RNMPC is more conservative than the NNMPC, which could lead to poorer performance in less severe situations. The optimization calculation-time of the RNMPC is about four times more than for the NNMPC. However, on the computer and software used here, this still means that the RNMPC is within the range of the real time requirements, with an average optimization time of less than 10 s.

The model applied in the NMPC and the one used for simulation are identical in this work. However, as discussed in Ersdal et al. (2013), it is believed that the positive features of the NMPC will be prominent also when some model mismatch is present. An advantage of the NMPC compared to the PI controllers is the way it is able to take into account the delays and different signal dispatching times. This is something that is difficult to do with other controllers.

6. CONCLUSION AND FURTHER WORK

A robustified NMPC which is based on a worst-case estimate of the deviation in produced wind power is designed, and simulations show that the RNMPC manages to fulfill the system constraints during severe disturbances, when the NNMPC and PI controller fails to do so. Under severe disturbances, the RNMPC also performs better and lower the use of the more expensive FCR and FRR at the cost of higher use of the cheaper RR. Under less severe disturbances, not resulting in violation of the system constraints, the NNMPC performs better due to the conservative nature of the RNMPC.

The results presented here illustrates how knowledge of the worst-case estimate of wind power production can be used to make a NMPC for FC more robust. A natural path for further work is to include model-uncertainty and evaluate robustness with regards to this, and also test the controller on a larger power system simulator.

REFERENCES

Andersson, J., Åkesson, J., and Diehl, M. (2012). CasADi – A symbolic package for automatic differentiation and optimal control. In S. Forth, P. Hovland, E. Phipps, J. Utke, and A. Walther (eds.), *Recent Advances in Algorithmic Differentiation*, volume 87 of *Lecture Notes in Computational Science and Engineering*, 297–307. Springer Berlin Heidelberg.

Bevrani, H. (2009). *Robust Power System Frequency Control*. Springer.

Bevrani, H., Hiyama, T., and Bevrani, H. (2011). Robust PID based power system stabilizer: Design and real-time implementation. *International Journal of Electrical Power & Energy Systems*, 33, 179–188.

Biegler, L.T. (2010). *Nonlinear Programming: Concepts, Algorithms, and Applications to Chemical Processes*. SIAM.

Cam, E. and Kocaarslan, I. (2013). Load frequency control in two area power system using fuzzy logic controller. *Energy Conversion Management*, 46.

ENTSO-E (2012). *Operational Reserve Ad Hoc Team Report*. Final Version.

Ersdal, A.M., Cecílio, I.M., Fabozzi, D., Imsland, L., and Thornhill, N.F. (2013). Applying model predictive control to power system frequency control. In *Proc. 2013 IEEE Innovative Smart Grid Technologies Europe*.

Fabozzi, D., Thornhill, N.F., and Pal, B.C. (2013). Frequency restoration reserve control scheme with participation of industrial loads. In *Proc. 2013 IEEE Grenoble PowerTech conf.*

Goodwin, G.C. and Medioli, A.M. (2013). Scenario-based, closed-loop model predictive control with application to emergency vehicle scheduling. *International Journal of Control*, 86(8), 1338–1348.

Grüne, L. and Pannek, J. (2011). *Nonlinear Model Predictive Control. Theory and Algorithms*. Springer.

Gross, G. and Lee, J.W. (2001). Analysis of load frequency control performance assessment criteria. *IEEE Transactions on Power Systems*, 16, 520–525.

Holttinen, H. (2004). *The impact of large scale wind power production on the Nordic electricity system*. Ph.D. thesis, Helsinki University of Technology.

Huang, R., Patwardhan, S.C., and Biegler, L.T. (2009). Multi-scenario-based robust nonlinear model predictive control with first principle models. *Computer Aided Chemical Engineering*, 27, 1293–1298.

Khodabakhshian, A. and Edrisi, M. (2008). A new robust PID load frequency controller. *Control Engineering Practice*, 16, 1069–1080.

Machowski, J., Bialek, J.W., and Bumby, J.R. (2008). *Power System Dynamics. Stability and Control*. Wiley.

Mohamed, T.H., Morel, J., Bevrani, H., and Hiyama, T. (2012). Model predictive based load frequency control design concerning wind turbines. *International Journal of Electrical Power & Energy Systems*, 43(1).

Nordel (2008). *Nordel Annual Statistics 1997-2008*.

Rawlings, J.B. and Mayne, D.Q. (2009). *Model Predictive Control: Theory and Design*. Nob Hill Publishing.

Scokaert, P. and Mayne, D. (1998). Min-max feedback model predictive control for constrained linear systems. *IEEE Transactions on Automatic Control*, 43(8), 1136–1142.

Shiroei, M., Toulabi, M.R., and Ranjbar, A.M. (2013). Robust multivariable predictive based load frequency control considering generation rate constraint. *International Journal of Electrical Power & Energy Systems*, 46, 405–413.

Singh, V.P., Mohanty, S.R., Kishor, N., and Ray, P.K. (2013). Robust H-infinity load frequency control in hybrid distributed generation systems. *International Journal of Electric Power & Energy Systems*, 46, 294–305.

Statnett (2012). Systemdrifts- og markedsutviklingsplan 2012. Technical report.

Venkat, A.N., Hiskens, I.A., Rawlings, J.B., and Wright, S.J. (2008). Distributed MPC strategies with application to power system automatic generation control. *IEEE Transactions on Control Systems Technology*, 16(6), 1192–1206.

Whitley, D. and Gjerde, O. (2011). LFC/AGC-Nordic and European perspective. In *Exchange of balancing services between the Nordic and the Central European synchronous systems*, 1–13.